

# Properties of host haloes of Lyman-break galaxies and Lyman-alpha Emitters from their number densities and angular clustering

Takashi Hamana<sup>1,2</sup>, Masami Ouchi<sup>3</sup>, Kazuhiro Shimasaku<sup>3,4</sup>, Issha Kayo<sup>5</sup>  
and Yasushi Suto<sup>4,5</sup>

<sup>1</sup> Institut d’Astrophysique de Paris, 98bis Boulevard Arago, F 75014 Paris, France

<sup>2</sup> National Astronomical Observatory of Japan, Mitaka, Tokyo 181-8588, Japan

<sup>3</sup> Department of Astronomy, School of Science, University of Tokyo, Tokyo 113-0033, Japan

<sup>4</sup> Research Center for the Early Universe (RESCEU), School of Science, University of Tokyo, Tokyo 113-0033, Japan

<sup>5</sup> Department of Physics, University of Tokyo, Tokyo 113-0033, Japan

Accepted \*\*\*\*\*; Received \*\*\*\*\*; in original form 2003 July 10

## ABSTRACT

We examine relation between three different populations of high-redshift galaxies and their hosting dark halos employing the halo model approach. Specifically we consider LBGs (Lyman-break galaxies) at  $z \sim 4$  and at  $z \sim 5$ , and LAEs (Lyman-Alpha emitters) at  $z \simeq 4.86$ , all from the Subaru Deep Field survey. We adopt a halo occupation function (HOF) prescription to parameterize the properties of their hosting halos and the efficiency of halo-dependent star formation. We find that all the three samples are well described by the halo model with an appropriate HOF. Comparing the model predictions with the observed number densities and the angular correlation functions for those galaxies, we obtain constraints on properties of their hosting halos. A possible picture emerging from the current analysis is that LBGs corresponds to a population of central cluster galaxy at the present epoch, and that the LAEs are less massive galaxies whose star formation is somehow triggered at outer regions of very massive halos. On the other hand, we also find that the observed behavior of the angular two-point correlation for LAEs may not fully match the above picture. This may provide a clue to understand the nature of LAEs via future observations.

**Key words:** cosmology: theory — galaxies: high redshift — galaxies: haloes — galaxies: formation — dark matter

## 1 INTRODUCTION

Multi-band color selection techniques (Steidel et al. 1996; 1998; Madau et al. 1996; Cowie & Hu 1998; Ouchi et al. 2001; 2003) have significantly increased high-redshift galaxy catalogs both in quality and in size. Since those high- $z$  galaxies are naturally expected to be progenitors of the present-day galaxies, their statistical analysis is of fundamental importance in understanding the formation and evolution history of galaxies. Actually, recent large high- $z$  galaxy catalogs allow one to estimate their luminosity functions and spatial correlation functions at different  $z$  with a reasonable accuracy (e.g., Steidel et al. 1999; Adelberger et al. 1998; Giavalisco & Dickinson 2001; Ouchi et al. 2001; 2003; Porciani & Giavalisco 2002).

In the standard scenario of structure formation, it is thought that dark matter halos are first formed via the gravitational amplification of initial small density fluctuations.

Subsequently baryonic gas trapped in a gravitational potential of the dark matter halo becomes sufficiently dense to cool and to form stars, and initial small systems experience repeated mergers to form larger galaxies. The formation process of halos involves gravity only, thus it is well understood from  $N$ -body simulations as well as simple but relevant analytical approximations such as the Press-Schechter model (Press & Schechter, 1974) and its extensions (Bond et al. 1991; Bower 1991; Lacy & Cole 1993; Mo & White 1996). The formation of galaxies, on the other hand, involves many complicated processes including hydrodynamics, radiative processes, star formation, and supernova feedback, and thus it is hard to solve in a reliable manner even using state-of-the-art numerical simulations. Therefore, a simplified or empirical model that describes essential physical processes is still a valuable tool to understand basic elements of the formation and evolution of galaxies.

This is why we attempt in what follows to apply an em-

pirical parameterized model that relates the galaxy number distribution to mass of the hosting dark matter halo. To be more specific, we explore statistical relations between two populations of high- $z$  galaxies and their hosting dark matter halos: (i) Lyman break galaxies (hereafter LBGs) which are isolated in a color–color diagram due to their UV continuum depression (Steidel et al. 1996; 1998; Madau et al. 1996; Adelberger et al. 1998; Ouchi et al. 2001) and (ii) Lyman  $\alpha$  emitters (LAEs) which are identified due to their strong Lyman  $\alpha$  emission from narrow band imaging (Cowie & Hu 1998; Hu, Cowie & McMahon 1998; Ouchi et al. 2003; Shimasaku et al. 2003). We consider three catalogs generated from the Subaru Deep Field survey data (Ouchi et al. 2001; 2003; Shimasaku et al. 2003); LBGs at  $z \sim 4$ , LBGs at  $z \sim 5$  and LAEs at  $z \simeq 4.68$ .

The major purpose of our current analysis is twofold; the first is to clarify differences of hosting halos for LBGs and LAEs. It is well known that these two populations exhibit different statistical properties, including the fact that LAEs are in general fainter and smaller, and are more strongly clustered than LBGs (Ouchi et al. 2003). These differences should retain information of their formation processes as well as environmental effects. The second is to examine differences between LBGs located at different redshifts ( $z \sim 4$  and  $\sim 5$ ). Combined with the previous analysis of LBGs at  $z \sim 3$  by Moustakas & Somerville (2001) and Bullock et al. (2002), our results would provide better understanding of the evolution of LBGs.

To do this, we employ the halo approach that attempts to model the spatial distribution of galaxies in a parameterized fashion. The key quantity in this approach is the halo occupation function (HOF) that describes statistical relations between galaxies and their hosting halos. We adopt a simple form for HOF motivated by the semi-analytic galaxy formation models (Benson et al. 2000; Kauffmann et al. 1999) as well as by hydrodynamic simulations (Yoshikawa et al. 2001; White, Hernquist & Springel 2002). Combined with models of the halo mass function and spatial clustering of halos, for which very accurate fitting functions are obtained from  $N$ -body simulations (Jing 1998; Sheth & Tormen 1999; Hamana et al. 2001; Jenkins et al. 2001), the halo approach predicts the spatial clustering of galaxies as well as the galaxy number density. Comparing these predictions with observed values, we obtain a constraint on the relation between galaxies and their hosting halo mass for different populations of galaxies. This methodology was first attempted by Jing & Suto (1998) for LBGs at  $z \sim 3$  using their halo catalogs from  $N$ -body simulations.

The outline of this paper is as follows. In section 2, we describe models and basic equations. In section 3, we summarize observational data that are used to put constraints on the model parameters. Results are presented in section 4, and Section 5 is devoted to summary and discussion.

Throughout this paper, we adopt a flat  $\Lambda$ CDM (Cold Dark Matter) cosmology with the matter density  $\Omega_m = 0.3$ , the cosmological constant  $\Omega_\Lambda = 0.7$ , the Hubble constant  $H_0 = 100h\text{km/s/Mpc}$  with  $h = 0.7$ , and the normalization of the matter power spectrum  $\sigma_8 = 0.9$ . We adopt the fitting function of the CDM power spectrum of Bardeen et al. (1986).

## 2 HALO APPROACH FOR GALAXY CLUSTERING

The basic idea behind the halo model that we adopt below has a long history (Neyman & Scott 1952; Limber 1953; Peebles 1974, 1980; McClelland & Silk 1977; and numerous recent papers referred to in this section). The model predictions have been significantly improved with the recent accurate models for the mass function, the biasing and the density profile of dark matter halos (Seljak 2000; Peacock & Smith 2000; Ma & Fry 2000). This approach has been applied to various problems in cosmological nonlinear clustering, galaxy clustering and weak lensing correlation (e.g., Sheth & Jain 1997; Komatsu & Kitayama 1999; Cooray, Hu & Miralda-Escude 2000; Cooray & Sheth 2002; Scoccimarro et al. 2001; Hamana, Yoshida & Suto 2002; Berlind & Weinberg 2002; Bullock, Wechsler & Somerville 2002; Moustakas & Somerville 2002; Takada & Jain 2003). In this section, we summarize several expressions which are most relevant to the current analysis. In particular, we mainly follow the modeling of Berlind & Weinberg (2002), Bullock et al. (2002) and Moustakas & Somerville (2002) in which readers may find further details.

We adopt a simple parametric form for the average number of a given galaxy population as a function of the hosting halo mass:

$$N_g(M) = \begin{cases} (M/M_1)^\alpha & (M > M_{\min}) \\ 0 & (M < M_{\min}) \end{cases} . \quad (1)$$

The above statistical and empirical relation is the essential ingredient in the current modeling characterized by the minimum mass of halos which host the population of galaxies ( $M_{\min}$ ), a normalization parameter which can be interpreted as the critical mass above which halos typically host more than one galaxy ( $M_1$ ; note that  $M_1$  may exceed  $M_{\min}$  since the above relation represents the statistically expected value of the number of galaxies), and the power-law index of the mass dependence of the efficiency of galaxy formation ( $\alpha$ ). We will put constraints on the three parameters from the observed number density and clustering amplitude for each galaxy population. In short, the number density of galaxies is most sensitive to  $M_1$  which changes the average number of galaxies per halo. The clustering amplitude on large angular scales ( $> 1'$ ) is determined by the hosting halos and thus very sensitive to the mass of those halos,  $M_{\min}$ . The clustering on smaller scales, on the other hand, depends on those three parameters in a fairly complicated fashion; roughly speaking,  $M_{\min}$  changes the amplitude,  $\alpha$ , and to a lesser extent  $M_1$  as well, changes the slope. Further detailed discussion may be found in Berlind & Weinberg (2002), Bullock et al. (2002) and Moustakas & Somerville (2002).

With the above relation, the number density of the corresponding galaxy population at redshift  $z$  is given by

$$n_{g,z}(z) = \int_{M_{\min}}^{\infty} dM \, n_{\text{halo}}(M, z) \, N_g(M), \quad (2)$$

where  $n_{\text{halo}}(M)$  denotes the halo mass function for which we adopt the fitting function of Sheth & Tormen (1999).

The galaxy two-point correlation function on small scales is dominated by contributions of galaxy pairs located in the same halo. We adopt the following model

(Bullock et al. 2002) for the mean number of galaxy pairs  $\langle N_g(N_g-1) \rangle(M)$  within a halo of mass  $M$ :

$$\langle N_g(N_g-1) \rangle(M) = \begin{cases} N_g^2(M) & \text{if } N_g(M) > 1 \\ N_g^2(M) \log(4N_g(M))/\log(4) & \text{if } 1 > N_g(M) > 0.25 \\ 0 & \text{otherwise.} \end{cases} \quad (3)$$

The above empirical model is motivated by previous results from the semi-analytic galaxy formation models (Benson et al. 2000; Kauffmann et al. 1999) which indicate that for  $N_g(M) > 1$  the scatter around the mean number of galaxies is Poissonian, while for  $N_g(M) < 1$  it becomes sub-Poissonian.

In the framework of the halo model, the galaxy power spectrum consists of two contributions, one from galaxy pairs located in the same halo (1-halo term) and the other from galaxy pairs located in two different halos (2-halo term). Assuming the linear halo bias model (Mo & White 1996), the 2-halo term reduces to

$$P_g^{2h}(k) = \frac{P_{\text{lin}}(k)}{n_{g,z}^2} \times \left[ \int dM n_{\text{halo}}(M) N_g(M) b(M) y(k, M) \right]^2, \quad (4)$$

where  $P_{\text{lin}}(k)$  is the linear dark matter power spectrum,  $b(M)$  is the halo bias factor (we adopt the modified fitting function of Sheth & Tormen 1999), and  $y(k, M)$  is the Fourier transform of the halo dark matter profile normalized by its mass,  $y(k, M) = \tilde{\rho}(k, M)/M$ . See, e.g., section 3 of Seljak (2000) for details. Here we assume that galaxies in halos trace the density profile of the underlying dark halos by Navarro, Frenk & White (1996; 1997), and adopt the mass-concentration parameter relation by Bullock et al. (2001) but with an appropriate correction (see Shimizu et al. 2003). Since the clustering on large scales is dominated by the 2-halo term, it is fairly insensitive to the assumption of galaxy distribution inside the hosting halo (Berlind & Weinberg 2002).

The 1-halo term is written as

$$P_g^{1h}(k) = \frac{1}{(2\pi)^3 n_{g,z}^2} \int dM n_{\text{halo}}(M) \langle N_g(N_g-1) \rangle(M) \times b(M) |y(k, M)|^p. \quad (5)$$

We choose  $p = 2$  for  $\langle N_g(N_g-1) \rangle > 1$  and  $p = 1$  for  $\langle N_g(N_g-1) \rangle < 1$  (Seljak 2000). Here we have assumed that in the limit of a small number of galaxies in one halo, one galaxy is located near the center of the halo. Therefore, in this case, the number of pairs is dominated by the central galaxy paired with a halo galaxy, and thus the probability of finding a galaxy pair is given by the single density profile of the galaxies within a halo.

Once the power spectrum of the galaxy population is specified, one can easily compute their angular two-point correlation function via the Limber projection (see e.g. chapter 2 of Bartelmann & Schneider 2001):

$$\omega(\theta) = \int dr q^2(r) \int \frac{dk}{2\pi} k P_g(k, r) J_0[f_K(r)\theta k], \quad (6)$$

where  $q(r)$  is the normalized selection function,  $J_0(x)$  is the zeroth-order Bessel function of the first kind, and  $r = r(z)$  is the radial comoving distance given by

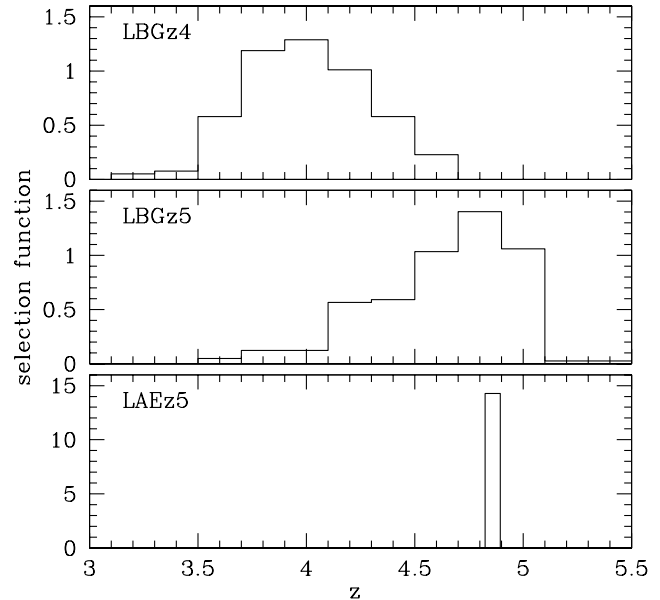


**Figure 1.** Selection functions as a function of redshift for LBGz4 (top), LBGz5 (middle) and LAEz5 (bottom).

$$r(z) = \frac{c}{H_0} \int_0^z \frac{dz}{\sqrt{\Omega_m(1+z)^3 + \Omega_\Lambda}} \quad (7)$$

for the spatially flat cosmology ( $\Omega_m + \Omega_\Lambda = 1$ ) as we consider in the present paper.

For a given selection function of observations, the average galaxy number density is

$$n_g = \frac{\int dz \frac{dV(r)}{dz} q(r) n_{g,z}(r)}{\int dz \frac{dV(r)}{dz} q(r)}, \quad (8)$$

where  $dV(r)/dz$  denotes the comoving volume element per unit solid angle:

$$\frac{dV}{dz} = r^2(z) \frac{dr}{dz} = \frac{c}{H_0} \frac{r^2}{\sqrt{\Omega_m(1+z)^3 + \Omega_\Lambda}}, \quad (9)$$

again for the spatially flat cosmology.

### 3 DATA

We use three different samples of galaxy populations from deep imaging data taken as part of the Subaru Deep Field (SDF) survey; LBGs at  $z \sim 4$  (LBGz4), LBGs at  $z \sim 5$  (LBGz5) and LAEs at  $z \simeq 4.86$  (LAEz5). Observational details of those samples are described in Ouchi et al. (2001; 2003; 2003b; 2003 in preparation), and thus we briefly summarize their basic features relevant for our comparison.

LBGz4s are selected from deep  $BRi'$  imaging data over a 543 arcmin<sup>2</sup> area in the SDF (Ouchi et al. 2003). The limiting AB magnitudes for the 3  $\sigma$  detection of an object in a 1''.8 diameter aperture are  $B = 27.8$ ,  $R = 27.1$  and  $i' = 26.9$ . They roughly correspond to the absolute magnitude of  $M_{1700} = -19.0 + 5 \log h$  at  $z = 4$ . A total of 1438 LBGz4 candidates are detected in a range of  $3.5 < z < 4.5$  (see top-panel of Fig. 1). Their number density is estimated to

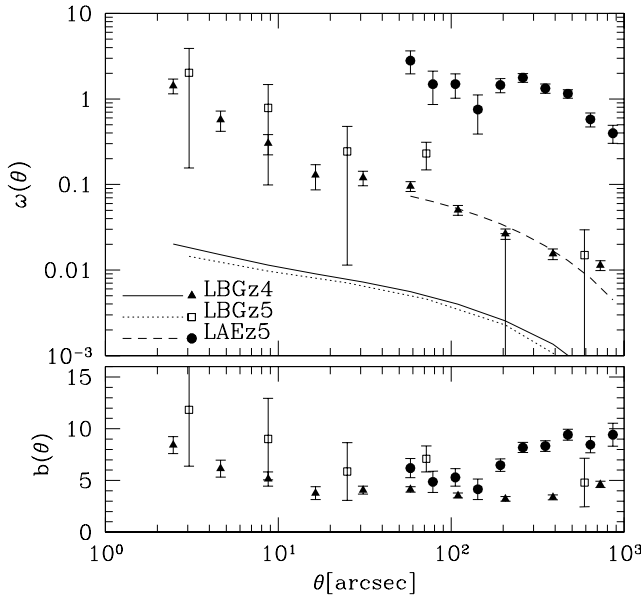


**Figure 2.** Angular two-point correlation functions (upper panel) and the corresponding bias parameter (lower panel) for three populations of high-redshift galaxies. Filled triangles, open squares, and filled circles represent the measured angular two-point correlation functions,  $w_g(\theta)$ , for LBGz4, LBGz5, and LAEz5, respectively. The model predictions for dark matter angular two-point correlation functions,  $w_{dm}(\theta)$ , in the  $\Lambda$ CDM cosmology with the same selection functions are plotted in curves; LBGz4 (solid line), LBGz5 (dotted line) and LAEz5 (dashed line). To compute them, the nonlinear fitting function of the CDM power spectrum by Peacock & Dodds (1996) is used. The biasing parameter is simply defined as  $b(\theta) \equiv \sqrt{w_g(\theta)/w_{dm}(\theta)}$ .

be  $n_{\text{LBGz4}} = (5.86 \pm 0.71) \times 10^{-3} h^{-3} \text{Mpc}^{-3}$ . The angular two-point correlation function is computed by the procedure described in Ouchi et al. (2001) and is plotted in Figure 2.

LBGz5s are selected from deep  $Vi'z'$  imaging data over a 616 arcmin<sup>2</sup> area in the SDF (Ouchi et al. 2003b; 2003 in preparation). The limiting AB magnitudes are  $B = 27.8$ ,  $V = 27.3$ ,  $R = 27.1$ ,  $i' = 26.9$ ,  $z' = 26.1$  for the 3  $\sigma$  detection in a 1''.8 diameter aperture. They roughly correspond to the absolute magnitude of  $M_{1700} = -19.7 + 5 \log h$  at  $z = 5$ . A total of 246 LBGz5 candidates are detected in a range of  $4.2 < z < 5.2$ . Their number density is estimated to be  $n_{\text{LBGz5}} = (8.05 \pm 4.96) \times 10^{-4} h^{-3} \text{Mpc}^{-3}$ .

LAEz5s are selected from the same data as for LBGz5s but an additional observation using a narrow band-filter (NB711, central wavelength of  $7126 \pm 4$  Å, FWHM bandwidth of  $73.0 \pm 0.6$  Å) was performed to identify LAEs at  $z \simeq 4.86$  (Ouchi et al. 2003). The limiting magnitude is NB711 = 26.0 for the 3  $\sigma$  detection in a 1''.8 diameter aperture. A total of 87 LAEz5 candidates are detected over  $4.83 \lesssim z \lesssim 4.89$ . Their number density is  $n_{\text{LAEz5}} = (3.01 \pm 1.94) \times 10^{-3} h^{-3} \text{Mpc}^{-3}$ .

The angular two-point correlation functions  $w_g(\theta)$  of those galaxy populations are plotted in Figure 2 together with those for dark matter,  $w_{dm}(\theta)$ , assuming the same selection functions for each galaxy sample. We define the biasing parameter as  $b(\theta) \equiv \sqrt{w_g(\theta)/w_{dm}(\theta)}$ . As was found earlier, LAEs exhibit stronger clustering than LBGs; we ob-

**Table 1.** Summary of observed properties, here the large scale bias is defined by  $b = \sqrt{w_g/w_{dm}}$  on scales  $60'' < \theta < 1000''$ .

Sample	number density [ $h^{-3} \text{Mpc}^{-3}$ ]	large scale bias
LBGz4	$(5.86 \pm 0.71) \times 10^{-3}$	$3 \sim 4.5$
LBGz5	$(8.05 \pm 4.96) \times 10^{-4}$	$5 \sim 7$
LAEz5	$(3.01 \pm 1.94) \times 10^{-3}$	$5 \sim 9$

tain  $b = 3 \sim 4.5$ ,  $5 \sim 7$  and  $5 \sim 9$  for LBGz4, LBGz5s and LAEz5, respectively, for  $60'' < \theta < 1000''$ .

## 4 RESULTS

### 4.1 Constraints on $M_{\text{min}}$ , $M_1$ , and $\alpha$

We estimate the range of allowed values for the three parameters,  $M_{\text{min}}$ ,  $M_1$ , and  $\alpha$  by considering the following  $\chi^2$  function constructed from the observed number density and the angular two-point correlation functions:

$$\chi^2(M_{\text{min}}, M_1, \alpha) = \sum_{\theta_{\text{bin}}} \frac{[\omega^{\text{obs}}(\theta_{\text{bin}}) - \omega^{\text{model}}(\theta_{\text{bin}})]^2}{\sigma_{\omega}^2(\theta_{\text{bin}})} + \frac{[\log n_g^{\text{obs}} - \log n_g^{\text{model}}]^2}{\sigma_{\log n_g}^2}, \quad (10)$$

where  $\sigma_{\omega}$  and  $\sigma_{\log n_g}$  are the statistical 1- $\sigma$  error in the measurements of the angular correlation function and the number density, respectively. In the above likelihood estimator, we take the logarithm of the galaxy number density instead of the number density itself, because the predicted galaxy number density varies logarithmically with  $M_1$ . Note that the present analysis does not take the cosmic variance into account although it may be important for relatively small survey volumes for those samples. Figures 3 to 5 show the  $\chi^2$  map on two-parameter planes after marginalizing over the remaining one parameter. The two-dimensional likelihood contours represent  $\Delta\chi^2 = 2.3$ , 6.17 and 11.8 which, if each bin of the correlation function is independent, should correspond to 68.3, 95.4 and 99.7% confidence levels (Press et al. 1986). Strictly speaking, however, the sampled correlation function bins are not completely independent, and these confidence levels should be regarded as approximate estimates.

Examine first the parameters for LBGz4s which are fairly strongly constrained by the observations (Fig. 3). Top-left panel shows the likelihood map on  $M_{\text{min}}-M_1$  plane. As pointed out earlier by Berlind & Weinberg (2002), Bullock et al. (2002), and Moustakas & Somerville (2002),  $M_1$  and  $M_{\text{min}}$  are mainly constrained by the number density and their clustering amplitude on large scales ( $\theta > 1'$ ), respectively. As Figure 2 shows, the observational uncertainty in the clustering amplitude for LBGz4s is fairly small and  $\delta n/n \sim 12\%$ . Thus we have relatively tight constraints on those two parameters.

The constraint on  $\alpha$  is weak because of the degeneracy with the other two parameters. Although the constraint on  $\alpha$  is not so strong, it is clear that the data favor  $\alpha < 1$  implying that the galaxy formation is less efficient for more massive halos.

Turn next to LBGz5 (Fig. 4). The constraints on this

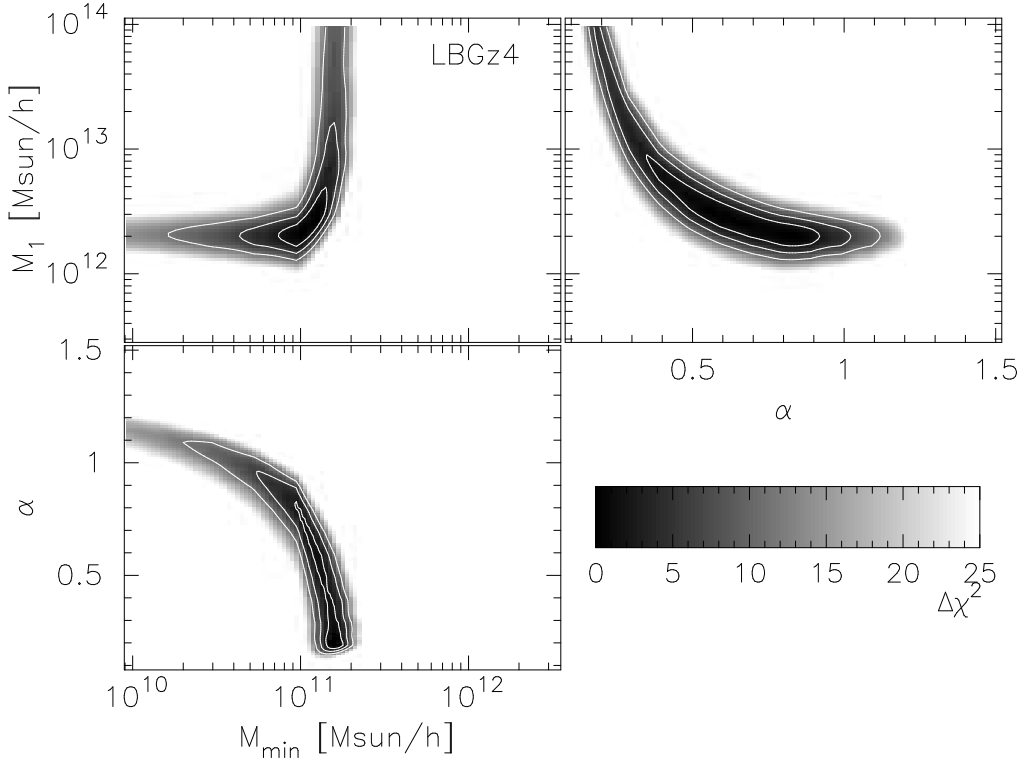


**Figure 3.** Confidence contour maps derived from  $\Delta\chi^2$  for LBGz4 on the two-parameter plane after marginalizing over the remaining one parameter. Top-left panel is on  $M_{\min}$ - $M_1$ , top-right on  $\alpha$ - $M_1$  and bottom-left on  $M_{\min}$ - $\alpha$ . A darker gray-scale indicates a lower  $\Delta\chi^2$  value (thus more likely). Contour lines indicate from inner to outer  $\Delta\chi^2 = 2.3, 6.17$  and  $11.8$ , which, if each bin of the correlation function is independent, correspond to  $68.3, 95.4$ , and  $99.73\%$  confidence levels, respectively. In the present analysis, these confidence levels should be understood as approximate estimates.

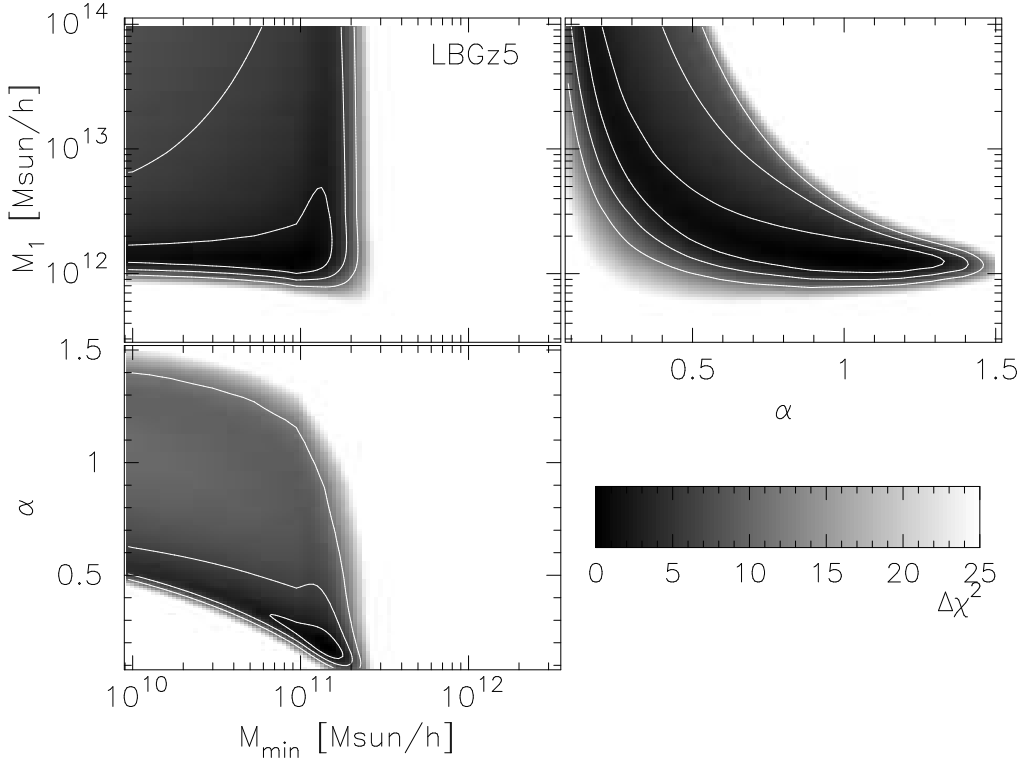


**Figure 4.** Same as Figure 3 but for LBGz5.

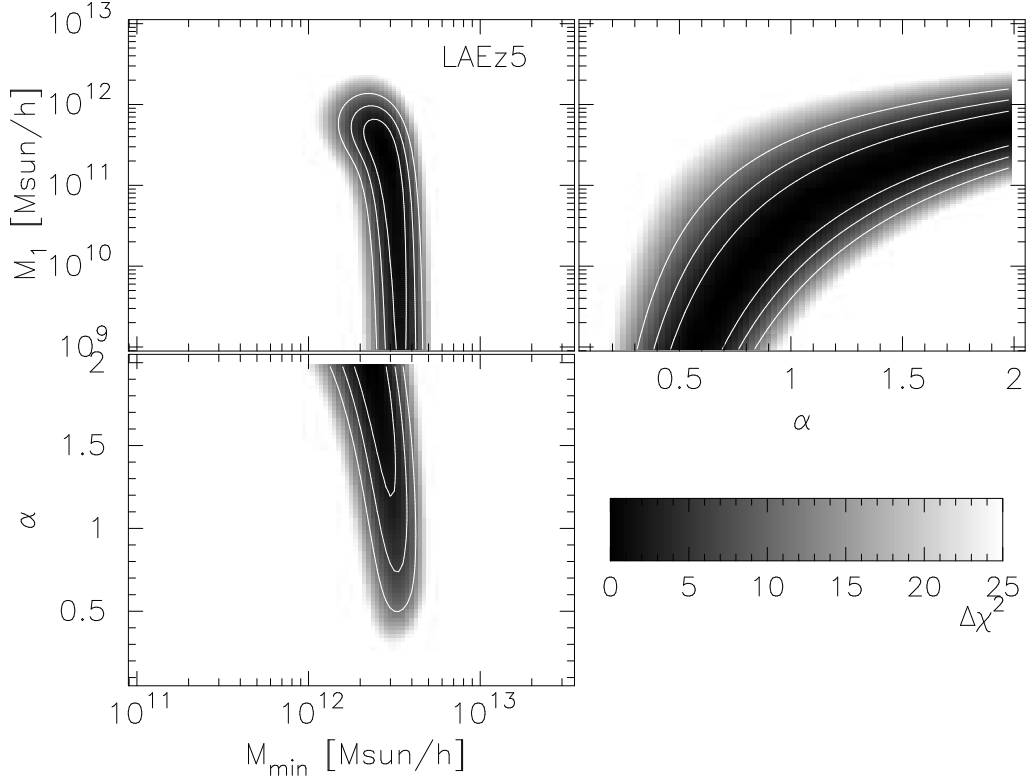


**Figure 5.** Same as Figure 3 but for LAEz5.

population are not so tight because of much larger uncertainties in the clustering amplitude (Fig. 2) and  $\delta n/n \sim 62\%$ . Nevertheless the constraints on the parameters for LBGz5s seem very similar to those for LBGz4, and we are not able to detect any significant changes of the parameters of LBGs between  $z = 4$  and 5.

Finally consider LAEz5s (Fig. 5) which have a relatively well determined correlation amplitude on large scales (Fig. 2) while their number density is rather uncertain,  $\delta n/n \sim 65\%$ . Therefore we barely obtain an upper limit of  $M_1 < 10^{12} h^{-1} M_\odot$ , while the value of  $M_{\min}$  is relatively well constrained as  $\sim 3 \times 10^{12} h^{-1} M_\odot$ . We do not have any strong constraints on  $\alpha$ , either, mainly due to the lack of information on the small-scale correlation function. Notice that although, in principle, *non-detection* of the small scale correlation function (in fact there are only a few LAEz5 pairs with the separation less than 50 arcsec) gives an important constraint on the spatial distribution of LAEz5, we do not use that information in our likelihood analysis but the likelihood function is computed from bins with non-zero signal only. Therefore, even if a preferred model predicts a detectable small scale correlation function, it is not contradictory to our likelihood analysis but suggests a need for a modification of the model of small scale spatial distribution of LAEz5s. As a matter of fact, this is indeed the case, and we will discuss this issue later in §4.4. Nevertheless there is an indication that LAEz5s prefer a larger value for  $\alpha$ , possibly  $\alpha > 1$ , than LBGs.

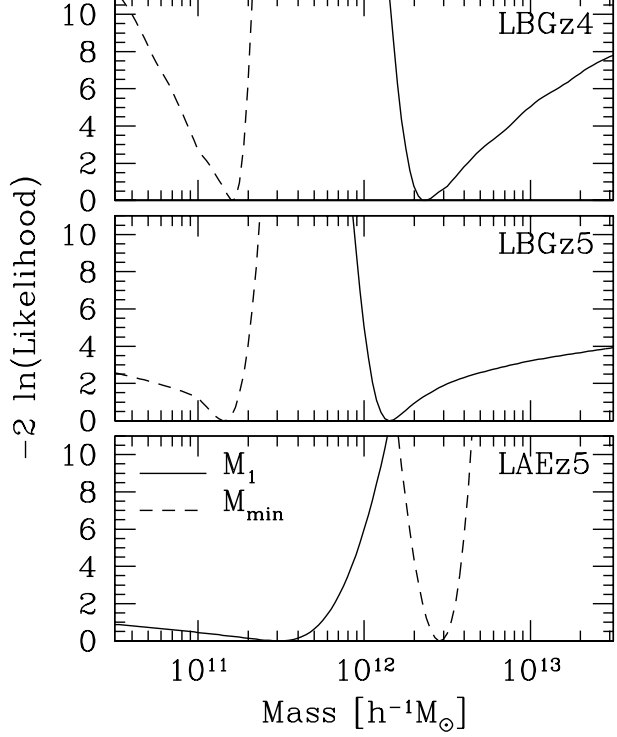


**Figure 6.** The likelihood functions ( $\Delta\chi^2$ ) for  $M_{\min}$  (dashed lines) and for  $M_1$  (solid lines) obtained after marginalizing over the other two parameters. Top is for LBGz4, middle is for LBGz5 and bottom is for LAEz5.

**Table 2.** The galaxy-number weighted average mass of hosting halo  $\langle M_{\text{host}} \rangle$  (in units of  $h^{-1} M_{\odot}$ ) and the expected number of galaxies per one halo  $\langle N_g \rangle$  for typical values of HOF parameters.

Sample ( $M_{\text{min}}$ , $M_1$ , $\alpha$ )	$\langle N_g \rangle$	$\langle M_{\text{halo}} \rangle$
LBGz4s ( $1.6 \times 10^{11}$ , $2.4 \times 10^{12}$ , 0.5)	0.38	$6.3 \times 10^{11}$
LBGz5 ( $1.4 \times 10^{11}$ , $1.4 \times 10^{12}$ , 0.5)	0.45	$4.5 \times 10^{11}$
LAEz5 ( $2.8 \times 10^{12}$ , $3.2 \times 10^{11}$ , 1.5)	50	$5.6 \times 10^{12}$
LAEz5 ( $2.8 \times 10^{12}$ , $3.2 \times 10^{11}$ , 1.0)	13	$5.0 \times 10^{12}$
LAEz5 ( $2.8 \times 10^{12}$ , $3.2 \times 10^{11}$ , 0.5)	3.6	$4.5 \times 10^{12}$

## 4.2 Mass of the hosting halos

Let us look into more carefully the hosting halo masses for the different galaxy populations. Figure 6 plots the likelihood functions ( $\Delta\chi^2$ ) for  $M_{\text{min}}$  (dashed lines) and for  $M_1$  (solid lines) after marginalizing over the remaining two parameters. The most interesting difference between the two populations is the fact that  $M_1 > M_{\text{min}}$  for LBGs while  $M_1 < M_{\text{min}}$  for LAEz5. According to the results of the above subsection, this difference can be understood as follows; LAEs exhibit stronger clustering than LBGs. In the framework of the halo model, this implies that the hosting halos for LAEs should be more strongly biased with respect to dark matter, and thus their minimum mass  $M_{\text{min}}$  should be larger. On the other hand, the average number density of LAEz5s is by a factor of 4 larger than that of LBGz5s. Since more massive halos become progressively rarer, the above two observational indications can be reconciled only by increasing the number of LAEz5s per halo relative to LBGz5s. Thus  $M_1$  for LAEz5 should be significantly smaller than that for LBGz5. This implies that the number of LAEz5 per halo is much larger than that of LBGz5.

The above result can be more quantitatively rephrased in terms of the following measures; the average mass of the hosting halo (member galaxy number weighted):

$$\langle M_{\text{host}} \rangle = \frac{\int_{M_{\text{min}}}^{\infty} dM M N_g(M) n_{\text{halo}}(M)}{\int_{M_{\text{min}}}^{\infty} dM N_g(M) n_{\text{halo}}(M)}, \quad (11)$$

and the expected number of galaxies per halo:

$$\langle N_g \rangle \equiv \frac{\int_{M_{\text{min}}}^{\infty} N_g(M) n_{\text{halo}}(M, z) dM}{\int_{M_{\text{min}}}^{\infty} n_{\text{halo}}(M, z) dM}. \quad (12)$$

Those are evaluated for typical sets of HOF parameters that we found in the previous subsection, which are summarized in Table 2. Since  $\alpha$  for LAEz5s is rather uncertain, we consider three cases ( $\alpha = 1.5$ , 1 and 0.5). The values of  $\langle M_{\text{host}} \rangle$  and  $\langle N_g \rangle$  clearly exhibit remarkable differences between LBGs and LAEs; typical masses of the hosting halos for LBGs are  $(5 \sim 6) \times 10^{11} h^{-1} M_{\odot}$ , and are by an order of magnitude smaller than those for LAEs ( $\sim 5 \times 10^{12} h^{-1} M_{\odot}$ ). The expected number of galaxies per halo is  $O(1)$  for LBGs but  $O(10)$  for LAEs. Thus LBGs have an approximate one-to-one correspondence to relatively less massive halos, while LAEs are preferentially clustered only around very massive halos.

## 4.3 Evolution of properties of the hosting halos for LBGs

Turn next to the evolution of the hosting halos for LBGs. Our current analysis indicates that the minimum halo mass  $M_{\text{min}}$  for LBGs is almost the same  $\sim 1.5 \times 10^{11} h^{-1} M_{\odot}$  at both  $z \sim 4$  and  $z \sim 5$ . The halo mass accommodating more than one galaxy,  $M_1$ , seems increasing as time although barely at a  $1-\sigma$  level.

The almost identical analyses by Moustakas & Somerville (2001) and Bullock et al. (2002) for  $z \sim 3$  LBGs (Steidel et al. 1998; Adelberger et al. 1998; Adelberger 2000) indicate that  $M_{\text{min}} = 1.3 \times 10^{10} h^{-1} M_{\odot}$  and  $M_1 = 6 \times 10^{12} h^{-1} M_{\odot}$  for  $\alpha = 0.8$ , and that  $M_{\text{min}} = (0.4 - 8) \times 10^{10} h^{-1} M_{\odot}$ ,  $M_1 = (6 - 10) \times 10^{12} h^{-1} M_{\odot}$  and  $0.9 < \alpha < 1.1$ , respectively. Taking account of the relatively large uncertainties in those estimates, their results are consistent with ours, and indeed the combined results may indicate an evolutionary trend of the smaller  $M_{\text{min}}$  and the larger  $M_1$  for decreasing  $z$ . While the different selection criterion at different redshifts may induce an artificial systematic effect in estimating hosting halo mass, this is not the case here. If the limiting flux of a sample is brighter, galaxies in the sample have a smaller number density and usually a higher clustering amplitude. This leads to increasing  $M_{\text{min}}$  and  $M_1$  simultaneously. However, the limiting absolute magnitudes for LBGz3s, LBGz4s and LBGz5s are  $M_{1700} = -19.3 + 5 \log h$ ,  $M_{1700} = -19.0 + 5 \log h$  and  $M_{1700} = -19.7 + 5 \log h$ , respectively. Therefore, it is very unlikely that the difference in the limiting magnitude solely accounts for the systematic (although weak) trends in  $M_{\text{min}}$  and  $M_1$ .

In summary, the hosting halos for LBGs are characterized as follows; (i)  $M_{\text{min}}$  is about  $\simeq 1.5 \times 10^{11} h^{-1} M_{\odot}$  both at  $z \sim 4$  and  $z \sim 5$ , while it becomes smaller at  $z \sim 3$  about  $M_{\text{min}} = (0.4 - 8) \times 10^{10} h^{-1} M_{\odot}$ . (ii)  $M_1$  increases with time,  $M_1 \simeq 1.4 \times 10^{12}$ ,  $2.4 \times 10^{12}$  and  $(6 - 10) \times 10^{12} h^{-1} M_{\odot}$  for  $z = 5$ , 4 and 3, respectively.

## 4.4 Predicted clustering of LBGs and LAEs

Finally let us compare in details the observed angular two-point correlations with the halo model predictions based on preferred parameters. Figures 7 and 8 show the comparison for LBGz4s and LBGz5. In plotting the model predictions, we adopt  $M_{\text{min}} = 1.6 \times 10^{11} h^{-1} M_{\odot}$ ,  $M_1 = 8 \times 10^{12} h^{-1} M_{\odot}$ , and  $\alpha = 0.75$  for LBGz4, and  $M_{\text{min}} = 1.5 \times 10^{11} h^{-1} M_{\odot}$ ,  $M_1 = 5 \times 10^{12} h^{-1} M_{\odot}$ , and  $\alpha = 0.75$  for LBGz5. Given the approximate and empirical nature of the halo model, the overall agreement is satisfactory.

Figure 9 shows the same plot for LAEz5 assuming  $M_{\text{min}} = 3 \times 10^{12} h^{-1} M_{\odot}$ ,  $M_1 = 1 \times 10^{11} h^{-1} M_{\odot}$ , and  $\alpha = 1.2$ . Notice again that the information of non-detection of small scale correlation function for LAEz5s was not used to compute the likelihood function, thus the model prediction on smaller scales shown by the thin curves should be understood as an extrapolation from the model constrained by the large scale correlation function and the number density, and suggests a need for modification of the model. Indeed Figure 9 clearly indicates a feature which may not be fully accounted for in the framework of the conventional halo model. Since a single halo accommodates approximately

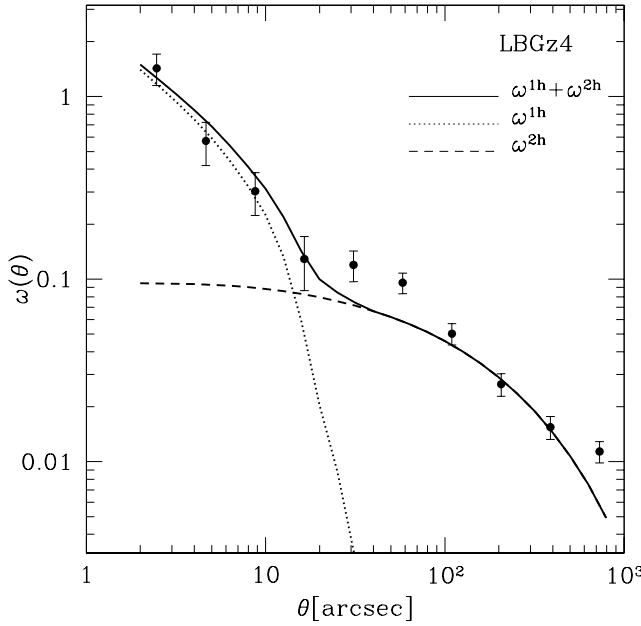


**Figure 7.** Comparison of the observed angular correlation function of LBGz4s with the model prediction assuming  $M_{\min} = 1.6 \times 10^{11} h^{-1} M_{\odot}$ ,  $M_1 = 8 \times 10^{12} h^{-1} M_{\odot}$ , and  $\alpha = 0.75$ .

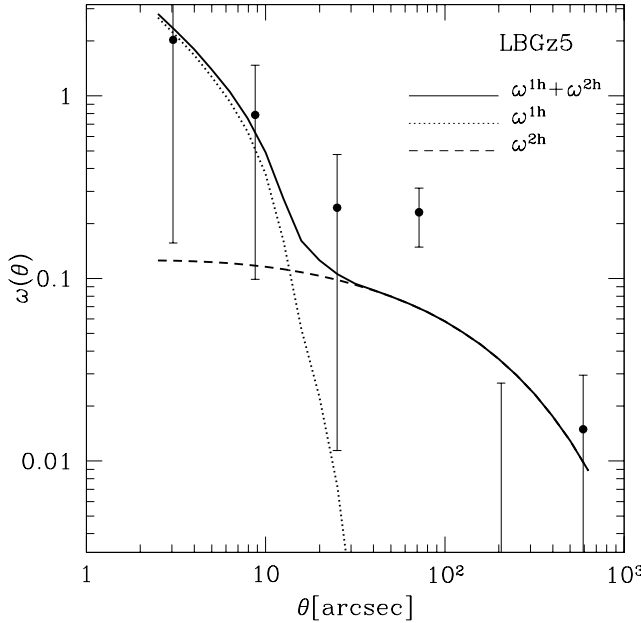


**Figure 8.** Same as Figure 7 but for LBGz5s assuming  $M_{\min} = 1.5 \times 10^{11} h^{-1} M_{\odot}$ ,  $M_1 = 5 \times 10^{12} h^{-1} M_{\odot}$ , and  $\alpha = 0.75$ .

$O(10)$  LAEs, one expects that the observed angular correlation would have strong signals on those scales where 1-halo terms dominate (specifically  $\theta < 40$  arcsec). In reality, we are not able to detect any signal for LAEs clustering on those scales.

In order to see if this feature may be ascribed to the small number of the LAEz5 sample that we consider, we create Mock LAEz5 samples out of  $N$ -body simulations of Jing & Suto (1998). We prepare an  $N$ -body output at  $z = 4.78$  and identify halos by the friend-of-friend algorithm with

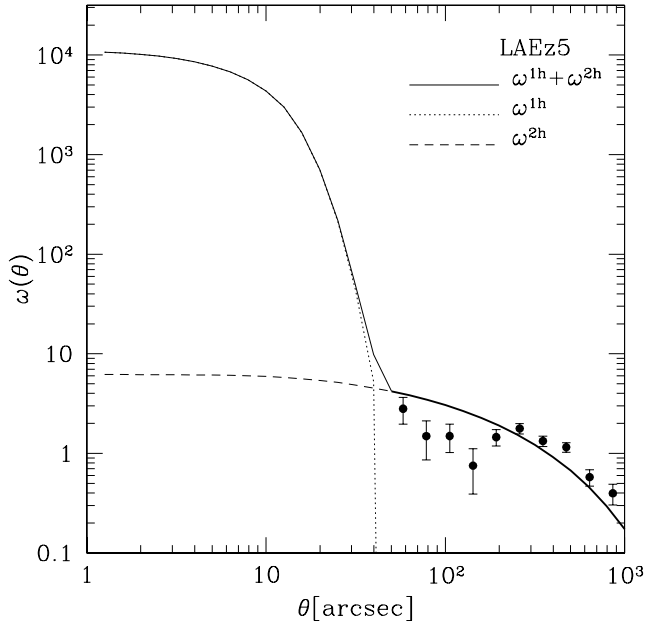


**Figure 9.** Same as Figure 7 but for LAEz5s assuming  $M_{\min} = 3 \times 10^{12} h^{-1} M_{\odot}$ ,  $M_1 = 1 \times 10^{11} h^{-1} M_{\odot}$ , and  $\alpha = 1.2$ . Note that the information on *non-detection* of small scale correlation function was not used to compute the likelihood function, thus the thin curves on small scales are not the model constrained from data on those scales, but should be understood as an extrapolation from the model constrained by the large scale correlation function and the number density.

linking length  $b = 0.164$ . Spatial positions of all member particles of each halo are stored in the halo catalog. Then, following the basic assumption of our halo model approach, we regard dark matter particles as candidates of ‘‘LAEs’’ and select ‘‘LAEs’’ from the member particles of the halos so as the number of the selected particles to follow the HOF with a parameter of  $M_{\min} = 1.0 \times 10^{12} M_{\odot}$ ,  $M_1 = 3.0 \times 10^{11} M_{\odot}$  and  $\alpha = 1.0$ . From this  $N$ -body output in which ‘‘LAEs’’ are embedded, we quarry some mock samples with  $25' \times 25' \times (\Delta z = 0.06)$  and calculate  $\omega(\theta)$  for each sample. The result is shown in Figure 10. The left panels show the distribution of the ‘‘LAEs’’ on the celestial sphere. We notice at a glance that the distribution is not similar to that of real LAEs (see Figure 5 in Ouchi et al. 2003). We can realize the difference more clearly comparing  $\omega(\theta)$  as shown in the right panels. In the mock samples we detect a clear and strong correlation on small scales less than  $50''$  as expected by the 1-halo term of the extrapolated model shown in Figure 9, which is not detected in the real sample. The error bars in these panels are estimated by the jackknife estimator which is not exactly the same as adopted in Ouchi et al. 2003. The discrepancy becomes worse if we use the best-fit parameter sets ( $M_{\min}$ ,  $M_1$ ,  $\alpha$ ) for HOF.

A possible way out of this difficulty is to assume that LAEs are associated with massive halos, but are located preferentially around the outskirts of the halos, maybe beyond their virial radius. This is in a sense inconsistent with the idea behind the halo model that we have adopted, and indicates an important direction toward improving the model.

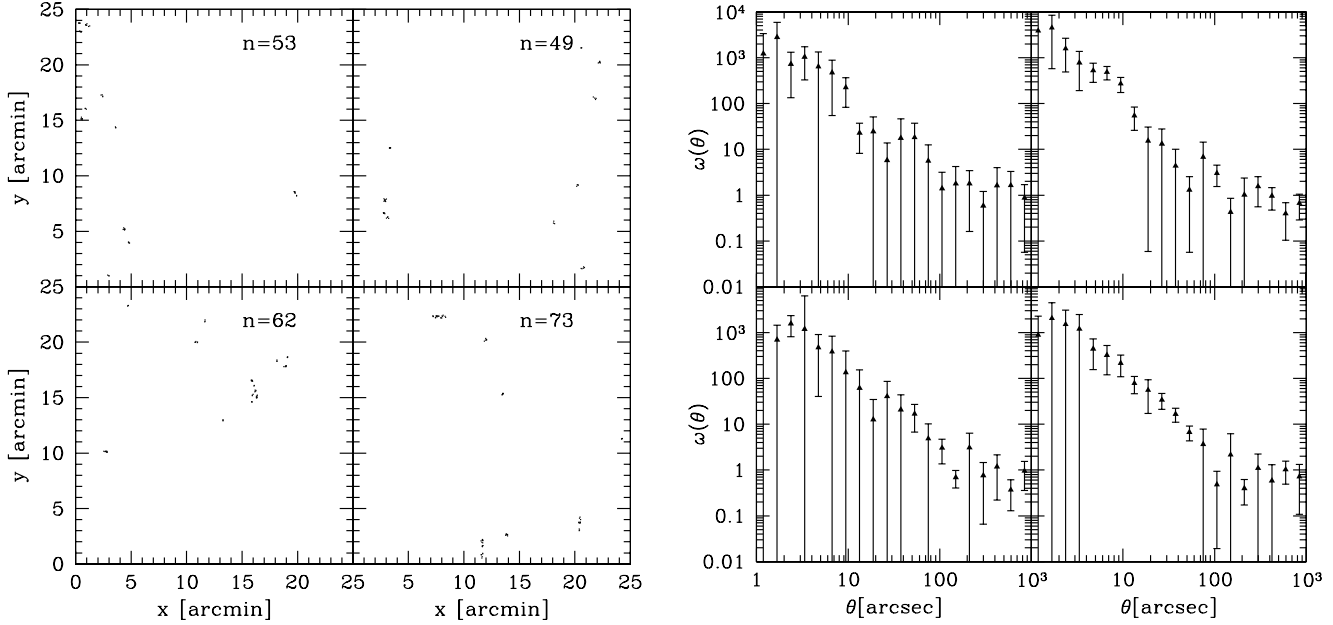


**Figure 10.** Distribution of mock LAEz5 samples on the celestial sphere (left) and angular correlation functions for them (right). The 4 panels on the left and right correspond to each other. The captions in the panels on the left mean the number of “LAEs” contained in each samples. The error bars on  $\omega(\theta)$  are estimated from 16 jackknife subsamples.

## 5 SUMMARY AND DISCUSSIONS

We have analyzed three high-redshift galaxy samples created from the Subaru Deep Field (SDF) survey project; LBGs at  $z \sim 4$  (LBGz4), LBGs at  $z \sim 5$  (LBGz5) and LAEs at  $z \simeq 4.86$  (LAEz5), and explored the implications of their number density and angular clustering in the framework of the halo occupation function (HOF).

Our major findings are summarized as follows;

(i) The three samples can be described by the halo model with an appropriate HOF in an approximate fashion.

(ii) The hosting halos for LBGz4s and LBGz5s are more massive than  $M_{\min} \sim 1.5 \times 10^{11} h^{-1} M_{\odot}$ . Since the expected number of LBGs per halo with  $M > M_{\min}$  is  $\sim 0.5$ , there is an approximate one-to-one correspondence between halos and LBGs. This is basically consistent with the results previously found for LBGs at  $z \sim 3$  (Mo, Fukugita 1996; Steidel et al. 1998; Jing & Suto 1998; Moustakas & Somerville 2001; Berlind & Weinberg 2002; Bullock et al. 2002).

(iii) On the other hand, this may also indicate that a large fraction of dark halos do not host LBGs brighter than  $M_{1700} \simeq -19$  mag. Nevertheless this does not mean that there is no galaxy in such halos. Franx et al. (2003) have found, at  $z \sim 3$ , red galaxies which do not have active star formation and so cannot be found by the Lyman break technique because of the very faint UV continuum emission. They estimate that the number density of such red galaxies is about half that of LBGs at the same redshift. Thus it may be the case that a fraction of the dark halos at  $z \sim 4-5$  host such red galaxies rather than bright LBGs that we discussed here.

(iv) In contrast, LAEs are hosted by more massive halos than those of LBGs and a single halo accommodates many LAEs, probably preferentially at its outer regions be-

yond its virial radius. In general, the strong Lyman  $\alpha$  emissions of LAEs suggest that they are star-bursting galaxies in which the star formation started very recently (e.g., Malhotra & Rhoads 2002; Schaefer 2003). The star formation in our LAEs may have been triggered recently by interactions with other LAEs or in the process of the gravitational infall to massive dark halos.

(v) The LBG samples at  $z \sim 3, 4$  and 5 discussed here have very similar limiting absolute magnitudes,  $M_{1700} \simeq -19$ . On the other hand, the minimum mass of their hosting halos seems decreasing as time, although its statistical significant is not strong. If true, this can be interpreted as that a measure of the star formation efficiency per unit dark matter mass,  $L_{1700}/M_{\text{halo}}$ , increases as time. This increase may be interpreted to suggest that cold gas gradually accumulates in LBGs, if the star formation rate is simply proportional to the amount of cold gas.

(vi) There is a weak indication for  $M_1$  to increase slightly as time. If real, this may be explained by the mutual merging of LBGs.

A possible picture emerging from the above results is that the LBGs correspond to a population of the central cluster galaxies at the present epoch, and that the LAEs are less massive galaxies whose star formation is somehow triggered at outer regions of very massive halos. As we have shown in the present paper, however, this picture may not be completely consistent with the behavior of the angular two-point correlation functions, and we plan to explore the issue in further details using the Mock catalogues from numerical simulations (Kayo et al. in preparation).

Another important issue to be addressed is the relation between LBGs and LAEs. According to the above simple picture, we expect that some fraction of massive halos should host an LBG in the central part and LAEs around its outer regions simultaneously. The discovery of such systems

is interesting in itself, and offers clear evidence supporting the picture.

## ACKNOWLEDGMENTS

T.H. and M.O. acknowledge supports from Japan Society for Promotion of Science (JSPS) Research Fellowships. I. K. gratefully acknowledges support from the Takenaka-Ikueikai fellowship. This research was also supported in part by the Grants-in-Aid from Monbu-Kagakusho and Japan Society of Promotion of Science (12640231, 13740150, 14102004, and 1470157). Numerical computations presented in this paper were carried out at ADAC (the Astronomical Data Analysis Center) of the National Astronomical Observatory, Japan (project ID: mys02a, yys08a).

## REFERENCES

Adelberger K. L., 2000, in ASP Conf. Ser. 200, Clustering at High Redshift, ed. A. Mazure, O. Le Févre, & V. Le Brun (San Francisco: ASP), 13

Adelberger K. L., Steidel C. C., Giavalisco M., Dickinson M., Pettini M., Kellogg M., 1998, *ApJ*, 505, 18

Bardeen J. M., Bond J. R., Kaiser N., Szalay A. S. 1986, *ApJ*, 304, 15

Bartelmann M., Schneider P., 2001, *Phys. Rep.*, 340, 291

Benson A. J., Cole S., Frenk C. S., Baugh C. M., Lacey C. G., 2000, *MNRAS*, 311, 793

Berlind A. A., Weinberg D. H., 2002, *ApJ*, 575, 587

Bond J. R., Cole S., Efstathiou G., Kaiser N., 1991, *ApJ*, 379, 440

Bower R. G., 1991, *MNRAS*, 248, 332

Bullock J. S., Kolatt T. S., Sigad Y., Somerville R. S., Kravtsov A. V., Klypin A. A., Primack J. R., Dekel A. 2001, *MNRAS*, 321, 559

Bullock J. S., Wechsler, R. H., Somerville R. S., 2002, *MNRAS*, 329, 346

Cooray A., Hu W., Miralda-Escude J. 2000, *ApJ*, 535, L9

Cooray A., Sheth R., 2002, *Phys. Rep.*, 372, 1

Cowie L. L., Hu E. M., 1998, *AJ*, 115, 1319

Franx, M. et al., 2003, *ApJ*, 587, L79

Giavalisco M., Dickinson M., 2001, *ApJ*, 550, 177

Hamana T., Yoshida N., Suto Y., 2002, *ApJ*, 568, 455

Hamana T., Yoshida N., Suto Y., Evrard A. E., 2001, *ApJ*, 561, L143

Hu E. M., Cowie L. L., McMahon R. G., 1998, *ApJ*, 502, L99

Jenkins A., Frenk C. S., White S. D. M., Colberg J. M., Cole S., Evrard A. E., Couchman H. M. P., Yoshida N., 2001, *MNRAS*, 321, 372

Jing Y. P., 1998, *ApJ*, 503, L9

Jing Y. P., Suto Y., 1998, *ApJ*, 494, L5

Kauffmann G., Colberg J. M., Diaferio A., White, S. D. M., 1999, *MNRAS*, 303, 188

Komatsu E., Kitayama T. 1999, *ApJ.*, 526, L1

Lacey C., Cole S. 1993, *MNRAS*, 262, 627

Limber D. N. 1953, *ApJ*, 117, 134

Ma C.-P., Fry J. N. 2000, *ApJ*, 543, 503

Madau P., Ferguson H. C., Dickinson M. E., Giavalisco M., Steidel C. C., Fruchter A., 1996, *MNRAS*, 283, 1388

Malhotra, S. & Rhoads, J. E. 2002, *ApJ*, 565, L71

McClelland J., Silk J. 1977, *ApJ*, 217, 331

Mo, H. J., Fukugita, M. 1996, *ApJ*, 467, L9

Mo, H. J., White, S. D.M. 1996, *MNRAS*, 282, 347

Moustakas L. A., Somerville R. S., 2002, *ApJ*, 577, 1

Navarro J., Frenk C., White S. D. M. 1996, *ApJ*, 462, 563

Navarro J., Frenk C., White S. D. M. 1997, *ApJ*, 490, 493

Neyman J., Scott E. L. 1952, *ApJ*, 116, 144

Ouchi M., et al., 2001, *ApJ*, 558, L83

Ouchi M., et al., 2003, *ApJ*, 582, 60

Ouchi M., et al., 2003b, Carnegie Observatories Astrophysics Series, Vol. 3: Clusters of Galaxies: Probes of Cosmological Structure and Galaxy Evolution , ed. J. S. Mulchaey, A. Dressler, and A. Oemler (Pasadena: Carnegie Observatories, <http://www.ociw.edu/ociw/symposia/series/symposium3/proceedings.html>)

Peacock J. A., Dodds S. J., 1996, *MNRAS*, 280, L19

Peacock J. A., & Smith R. E. 2000, *MNRAS*, 318, 1144

Peebles P. J. E. 1974, *A&A*, 32, 197

Peebles P. J. E., 1980, The Large-Scale Structure of the Universe Princeton Univ. Press, Princeton, NJ

Porciani C., Giavalisco M., 2002, *ApJ*, 565, 24

Press W. H., Flannery B. P., Teukolsky S. A., Vetterling W. T., 1986, Numerical Recipes (Cambridge: Cambridge Univ. Press)

Press W. H., Schechter P., 1974, *ApJ*, 187, 425

Schaerer D., 2003, *A&A*, 397, 527

Scoccimarro R., Sheth R. K., Hui L., Jain B., 2001, *ApJ*, 546, 20

Seljak U. 2000, *MNRAS*, 318, 203

Sheth R. K., Jain B.. 1997, *MNRAS*, 285, 231

Sheth R. K., Tormen G., 1999, *MNRAS*, 308, 119

Shimasaku K. et al., 2003, *ApJ*, 586, L111

Shimizu, M., Kitayama, T., Sasaki, S., Suto, Y., 2003, *ApJ*, 590, 197

Steidel C. C., Giavalisco M., Pettini M., Dickinson M., Adelberger K. L., 1996, *ApJ*, 461, L17

Steidel C. C., Adelberger K. L., Dickinson M., Giavalisco M., Pettini M., Kellogg M., 1998, *ApJ*, 492, 428

Steidel C. C., Adelberger K. L., Giavalisco M., Dickinson M., Pettini M., 1999, *ApJ*, 519, 1

Takada M., Jain B., 2003, *MNRAS*, 340, 580

White M., Hernquist L., Springel V., 2002 *ApJ*, 580, 634

Yoshikawa K., Taruya A., Jing Y.-P., Suto Y., 2001, *ApJ*, 558, 520